International Journal on Interactive Design and Manufacturing (IJIDeM)
https://doi.org/10.1007/s12008-024-02082-9

ORIGINAL ARTICLE

An advanced study on the application of artificial neural networks in the abrasive waterjet machining of titanium nanocomposites

T. S. Krishna Kumar[1] · **Ajay Kumar Kaviti**[2]

Received: 27 April 2024 / Accepted: 18 August 2024

Abstract
Titanium metal matrix composites (TiMMCs) are challenging to process because of hard Titanium particles. Increased cutting speed results in lower roughness values and longer tool life when grinding or turning. To solve this issue, artificial neural networks are employed in this study to forecast the geometrical properties of a microchannel created by abrasive water jet machining titanium-metal matrix composites (AWJM). This work determines the ideal values for four AWJM control parameters for cutting TiMMCs: Water fly mass, distance from water and object, stream rate, and navigation speed. Artificial Neuro-Fuzzy Logic Algorithm is used to achieve the desired process outputs (responses)—material ejection rate, cut surface roughness, kerf width, and kerf point. Interaction plots are generated to examine further how changing one or more AWJM process parameters affects the measured responses, and the analysis of variance is used to isolate the contributions of each process variable. The roughness of the cut surface and rate of material ejection, which is predominantly influenced by standoff distance, speed of navigation, and titanium nitride particles, were shown to be the AWJM variables that the proposed model was most successful in predicting and optimizing. The abrasive machining and optimization outcomes give a data foundation for many industrial applications. The results were validated by doing the confirmation test with optimized cutting parameters.

Keywords Abrasive waterjet cutting · Artificial neural networks (ANN) · Titanium metal matrix composites

1 Introduction

A titanium alloy matrix is the titanium metal matrix composite (TiMMC) foundation. It is reinforced with fibers, particles, or whiskers to give them extraordinary qualities, including high specific strength, high specific modulus, high-temperature resistance, and potential weight reduction. TiMMCs have replaced Ni-based alloys in aerospace applications for 30 years [1, 2]. Waterjet machining is one of the machining techniques that can process hard materials and delicate components with great precision. This makes it worthwhile in automobiles, renewable vitality, aviation, therapeutic gadgets, etc. [3–6].

The development of exceptional, cutting-edge technology for abrasive water jet machining (AWJM) is receiving much attention. As with any manufacturing process, there are downsides to the creation of abrasive jets. These include secondary erosive wear, abrasive fouling, taper profile, jet diffusion, inappropriate kerf geometry, and so on [7, 8]. Water fly mass, water jet angle of attack, angle of contact, feed rate, abrasive particle density, machining time, abrasive particle mass flow rate, and distance are the main determinants of abrasive jet machining [9, 10].

2 Related works

The rate of material rejection (MRR), roughness of the cut surface (Ra), kerf width, and kerf point are frequently used to measure the performance of machining operations. The performance of waterjet penetration in AWJM in aluminium–silicon carbide composites is primarily influenced by the speed of navigation and waterjet pressure [11, 12]. As

✉ T. S. Krishna Kumar
krishxxx99@gmail.com

Ajay Kumar Kaviti
ajaykumar_k@vnrvjiet.in

[1] Department of Automobile Engineering, VNR Vignana Jyothi Institute of Engineering and Technology, Hyderabad, Telangana, India

[2] Department of Mechanical Engineering, VNR Vignana Jyothi Institute of Engineering and Technology, Hyderabad, Telangana, India

Published online: 16 September 2024

a result of being machined, TiMMCs likely emit particles and severely wear down the tools. During the machining of TiMMCs in various lubricated modes, a recent study examined dust formation at the micro- and nanoscale. Although cutting speed has little effect on the specific surface concentration and mass concentration of ultrafine particles, it significantly impacts the generation of fine particles (2.5 M aerodynamic particle diameter or smaller) (size range of 0.1 M). Turning with lubricated tools reduces particle emission, as predicted, and coated inserts with high flow rates (300 ml/min) emit less ultrafine particles than their uncoated counterparts. [13, 14]. The roughness of the ground can also be affected by the concentration of reinforcing particles in the composite. The roughness of MMCs' surface is influenced by the number of reinforcing particles used [15–17]. The roughness does, however, lessen with TiMMCs. The matrix and particle composition likely contribute to the observed asymmetry in the roughness trend. Titanium carbide (TiC) particles are more durable than silicon carbide (SiC) particles, while titanium alloy (Ti6 Al4V) is more malleable than an aluminum alloy (Al alloy). Grooves and clusters can't form on TiC particles' surfaces. The rugged character of TiC particles encourages detachment rather than breaking, which helps to reduce roughness [18–23]—an analysis of how ANN is used in traditional machining to forecast the roughness of the cut surface.

According to the literature that is currently accessible, ANN's use for atypical machining processes is underdeveloped, and its application to AWJM is relatively limited. ANN provides a better method for estimating the process parameters based on the selection of the most crucial and advantageous values of the parameters, as shown by reports on the prediction of roughness of the cut surface and jet velocity for a given pressure, rate of abrasive mass stream, and thickness of the target material. With the help of numerical models, Yang's reports can be used to assess the AWJM technique's cutting capacity for a range of engineering materials [24–28]. The report on granite machining includes a study of the outcomes from empirical modeling and parameter optimization utilizing a hybrid strategy. The effectiveness of abrasive waterjet machining was measured using ANN. Neural networks provide an overview of unconventional machining techniques for abrasive waterjet cutting. The application of micro-channel property prediction at extremely high navigation speeds is covered in the current work. The neural network systems mentioned are versatile and can be used in different AWJM applications to enhance machining performance and efficiency [29, 30]. The utilization of high-pressure waterjet help has substantially enhanced the longevity of tools [31]. In this paper, experiments are carried out with AWJM to improve the tool's life.

Table 1 Properties of titanium

S.No	Element properties	Titanium
1	Physical state	Solid
2	Melting point	1667 °C
3	Initial boiling point and boiling range	3287 °C
4	Water solubility	at 20 °C insoluble
5	Density	4,5 g/cm^3 at 20 °C

3 Proposed methodology

The AWJM employed in the research projects is capable of producing a maximum working pressure of 400 MPa and a maximum pump capacity of 20 hp. The water jet travels at a high velocity of 900 m/s, which is a 3 Mach number. Figure 1a shows the experimental setup, and Fig. 1b shows the machined components.

Sigma Aldrich purchases titanium, whose properties are shown in Table 1. The material being utilized for the actual product is a composite of TiMn metal hydrides. The measured dimensions of an 8-mm-thick TiMMC are 250 mm. The AWJM method produced a clean 30-mm-long through-cut.

Figure 2 shows four AWJM process control parameters, including water fly mass, distance between water and object, steam rate, and navigation speed, after a meticulous selection technique.

The impact angle and focusing length have been held steady at 90 degrees and 0.76 mm throughout the machining process. The abrasive particle is a TiMMC with a mesh size of 80 (or 165 mm in length). The cutting head has been moved with a precision of 0.025 mm, and the nozzle has a diameter of 0.70 mm. MARR, SUR, KEW, and KEA are the four performance indicators chosen to assess the AWJM process's machining efficacy on TiMMC composites. Using Eq. (1), we can determine that MRR equals the material removed from the workpiece in one machining cycle. Using the roughness of the cut surface tester, we determined the SR value by averaging the results of three separate runs on the top, middle, and bottom of the machined surface of TiMMC composites. Top kerf width (TKEW) and bottom kerf width (BKEW) were measured using a 100X optical microscope at three positions along the cut length on both the top and bottom surfaces. After determining the sum of the two, we have the KEW. The Kerf taper, often known as KEA (Θ), is an essential measure of the precision of machined parts, which has been calculated using Eq. (2).

$$MARR = KEW \times TUS \times TH \tag{1}$$

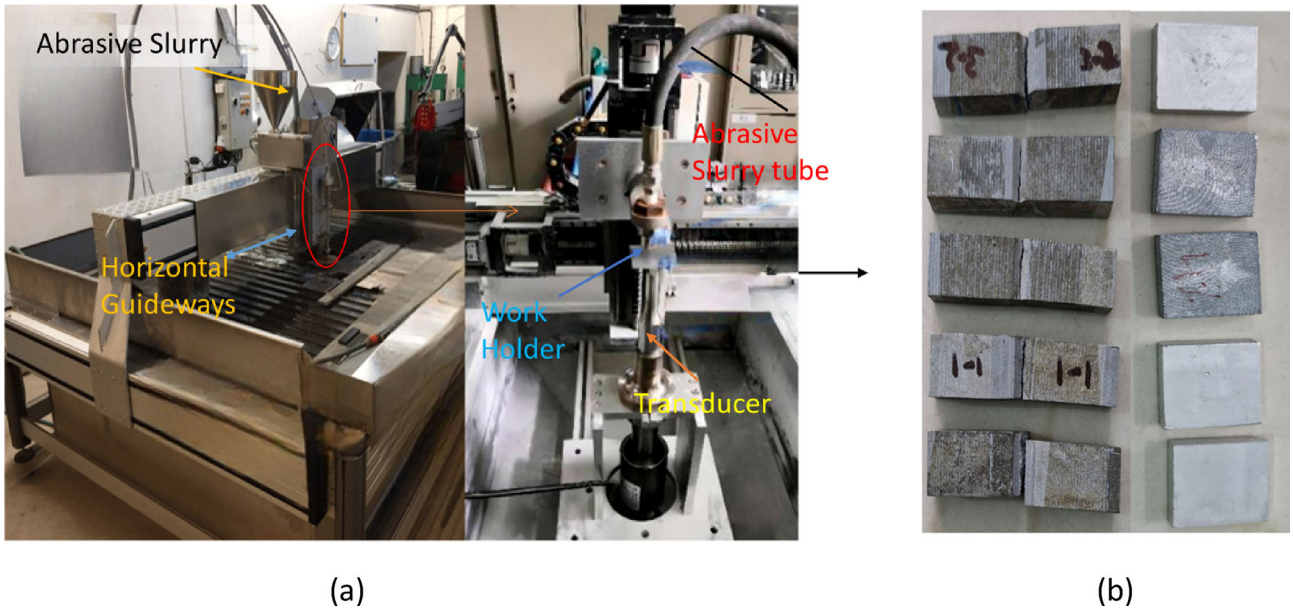

Fig. 1 **a** Experimental setup of abrasive water jet machining. **b** Machined components

Fig. 2 ANN model

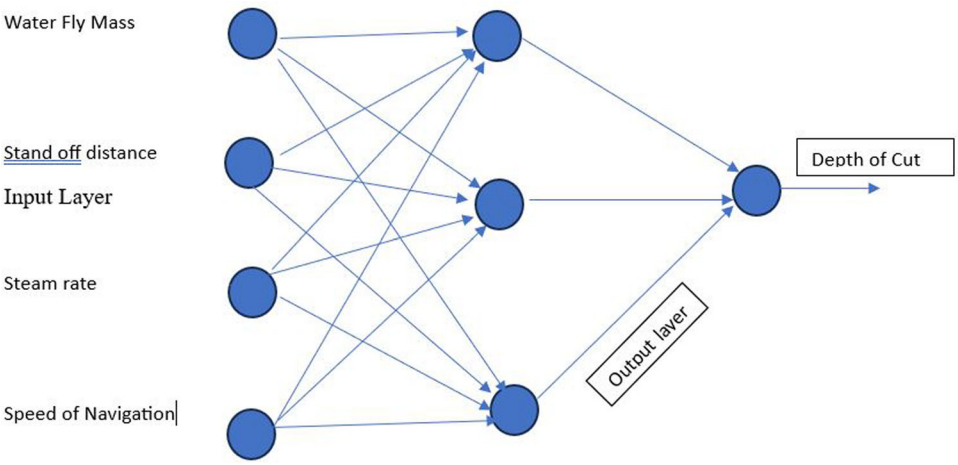

$$\theta = \tan^{-1}\left(\frac{TH_{KEW} - B_{KEW}}{2TH}\right) \tag{2}$$

3.1 An artificial neural fuzzy logic algorithm (ANFLA)

Developing a matrix of choices containing n criteria (responses) and alternative answers is the first stage in the ANFLA procedure. The methodology starts with experimental trials of the ANFLA. Figure 3 provides a comprehensive breakdown of the ANFLA application procedure, detailing each stage.

Step 1: Establishing a baseline for the matrix of choices.

Eliminating variability and making the dataset dimensionless requires normalizing the elements of the matrix of choices. Specifically, we need to put each component into a range between 0 and 1 that is consistent with the remainder of the range.

The following equations can be used, with care given to the sort of quality feature being analyzed: For those of you who believe the bigger, the better!

If the bigger-is-better kind.

$$c_{ij}^{*} = \left(c_{ij} - \min c_{ij}\right)/(\max c_{ij} - \min c_{ij}) \tag{3}$$

where i = 1,2, 3….m; j = 1,2, 3…n.

To get the best results, go for the smallest size possible.

$$c_{ij}^{*} = \left(maxc_{ij} - c_{ij}\right)/(\max c_{ij} - \min c_{ij}) \tag{4}$$

c_{ij}, c_{ij}^{*} are the measured and normalized values for the ith alternative for the jth criterion.

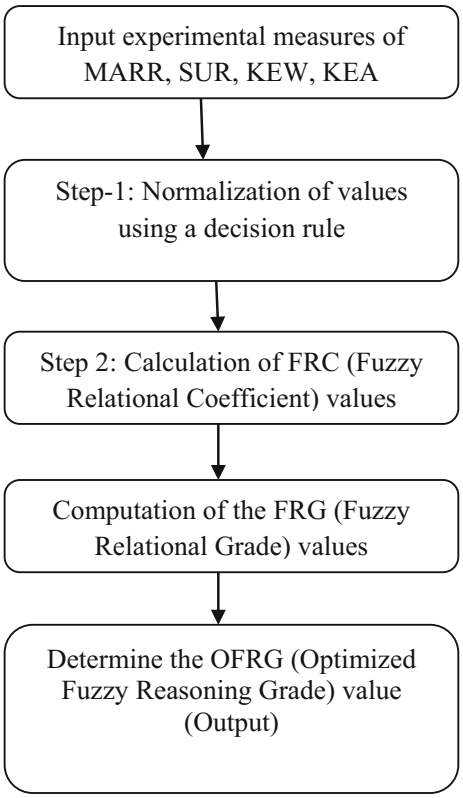

Fig. 3 A proposed ANFLA application process framework

Step 2: Calculation of relevant FRC (Fuzzy Relational Coefficient) values.

We can derive the FRC values from the normalized data for all responses by Eq. (5). They represent the relationship between the optimal (target) and actual normalized results.

$$\rho_{ij} = (\gamma_{min} + \beta\gamma_{max})/\left(\gamma_{ij}^{0} + \beta\gamma_{max}\right) \tag{5}$$

where γ_{ij}^{0} is the variation between c_{ij}^{0} (ideal sequence) and c_{ij}^{*}. Contrarily, β is the differentiating coefficient, and it can take on values between 0 and 1, with 0.5 being the most optimal. To a large extent, it determines whether the range for FRC values widens or narrows. In addition, γ_{min} and γ_{max} denote the global minimum and maximum values in a given data set. A larger FRC number indicates a closer potential solution.

Step 3: Determination of FRG values via calculation.

Now, we compute the FRG values by averaging the FRCs for each criterion concerning each alternative, and the results are shown in Fig. 4.

$$F_i = \frac{1}{n}\sum_{j=1}^{n}\rho_{ij} \tag{6}$$

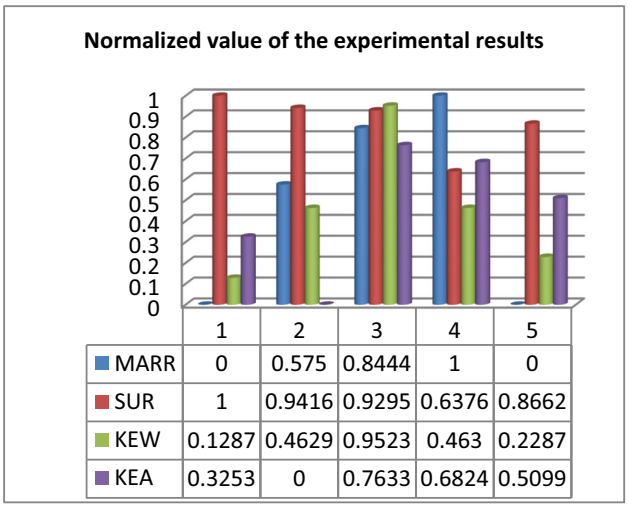

Fig. 4 Normalized values of the experimental results

For each given issue, the solution with the highest FRG value stands out as superior to all others. The experimental information needed to determine the FRC and FRG is shown in Fig. 5. The experimental findings are normalised to a range of 0–1 using either Eqs. (3) or (4), depending on the quality feature being addressed. Figure 5 displays the results of calculating the FRC and FRG for each experimental trial using the normalised data and the corresponding Eqs. (5) and (6). The third experiment with the highest FRG value was chosen as the optimal one. However, a fuzzy logic method boosts the solution's superiority and lessens the experimental findings' uncertainty and fuzziness.

3.2 Modelling with fuzzy-based rules

The Fuzzy Set Theory was developed primarily to resolve disagreements brought on by erroneous data when trying to reach a consensus on a course of action. In this paper, we combine ANFLA with fuzzy logic to remove the doubts that arise while weighing the relative merits of higher and smaller values for quality indicators. Fuzzy membership functions translate qualitative phrases like "low," "mid," "high," etc., into quantitative values for application in fuzzy set theory. A fuzzy set can be considered a collection of membership functions, where each membership function maps an element x into a set of objects, X, and the resulting mapping is a natural integer R between 0 and 1. Using fuzzy logic, the ambiguity of neuro theory can be eliminated. In other words, a fuzzy multi-performance instrument can be made using this technique, also known as neuro-fuzzy logic. The fuzziness near the center method is typically employed to convert the multi-response fuzzy value to the crisp value of OFRG.

$$OFRG = \frac{\sum F\mu_{F_0}(F)}{\sum \mu_{F_0}(F)} \tag{7}$$

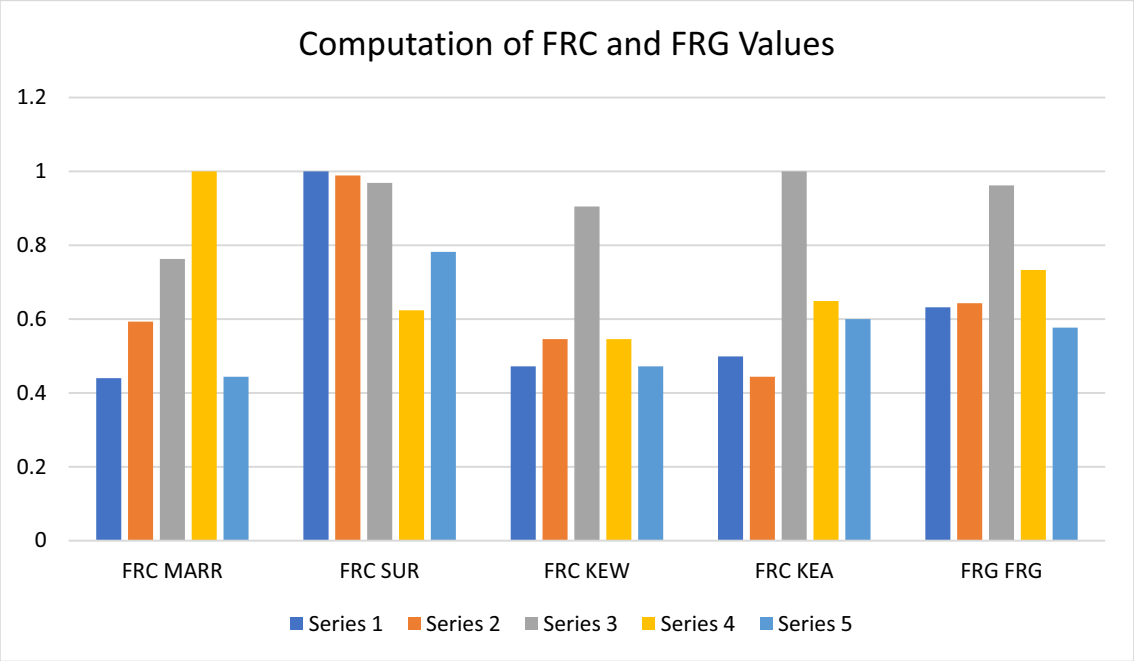

Fig. 5 Computation of FRC and FRG value

After, all uncertainties and ambiguities in the empirically observed data have been removed, the OFRG values can be rated from best to worst, with the best choice being selected. Ultrasonic-assisted electrical release machining, warm penetrating, and many others can all benefit from the ANFLA method combined with fuzzy logic, as it is a straightforward and effective strategy for addressing complex multi-criteria problems involving the identification of optimal parametric combinations. To find the perfect spot for all the variables in the AWJM process, this work uses a multi-response optimization method, namely an artificial neural-fuzzy approach.

3.3 Artificial neural fuzzy approach

This article describes how an artificial neural-fuzzy system was used to determine the optimal combination of processing parameters for AWJM on TiMMCs. An analysis is carried out to isolate the effect of each process parameter on the OFRG results. Table 2 shows the calculated OFRG value of the response.

In addition, the surface plots are created based on a regression equation that links the input parameters to the estimated OFRG values.

The impact of the AWJM process parameters on the results is also shown through interaction plots, as shown in Fig. 6.

Table 3 displays the results of variance analyses performed on the calculated OFRG values. A factor's p-value must be less than or equal to 0.05 (p 0.05) to be considered statistically significant. With 60.8% of the variance in OFRG values

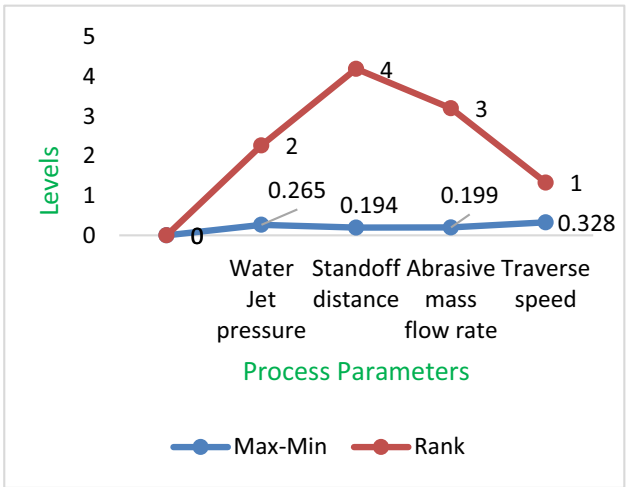

Fig. 6 Interaction plots of the calculated OFRG value

attributable to the traversal speed, it is evident that this is the most crucial control parameter.

3.4 Validation test

To verify whether the Neurofuzzy method-based approach is successful in determining the optimal parameters for the AWJM process under discussion, we calculate the predicted

Table 2 Response table for the calculated OFRG value

Process parameter	Levels			Max–Min	Rank
	1	2	3		
Water fly mass	0.741	0.687	0.588	0.265	2
Standoff distance (mm)	0.645	0.644	0.728	0.194	4
Steam rate	0.608	0.599	0.699	0.199	3
Speed of navigation (mm/min)	0.567	0.666	0.784	0.328	1

Table 3 Analysis results of OFRG values

Process parameter	F value	*p* value	% contribution
Water fly mass	7.47	0.176	36.67
Standoff distance	2.95	0.358	8.5
Steam rate	1.13	0.905	10.4
Speed of navigation	13.76	0.135	60.98

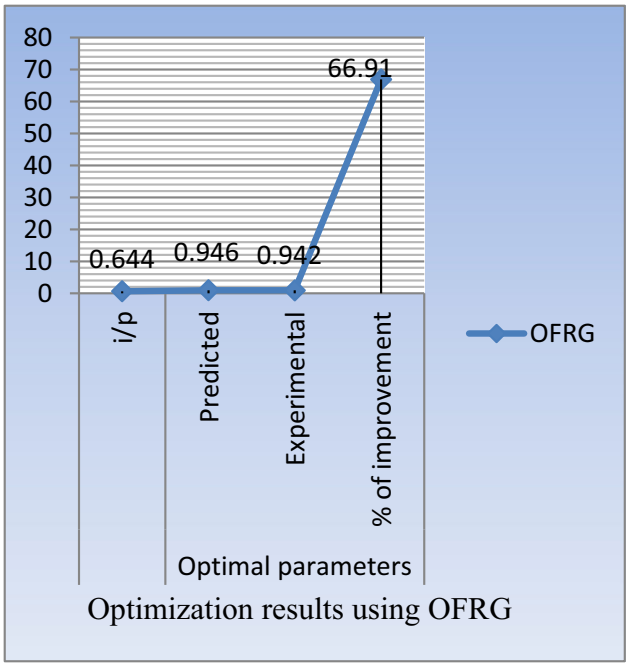

Fig. 7 Optimization results using OFRG

OFRG (OFRGp) value for this combination using Eq. (8).

$$OFRG_p = OFRG_m + \sum_{i=1}^{n} (\overline{OFRG_i} - OFRG_m) \quad (8)$$

OFRGi denotes the ideal level of the examined process parameters. The mean OFRG value is $OFRG_m$, where n is the total number of experimental trial runs, and $OFRG_i$ is the mean OFRG value.

OFRG is higher than in Fig. 7, established for the first machining condition. This step involves running a test to verify the derived optimal parametric blend.

Table 4 shows how the measured responses differ between the default and best parameter values. Using the data in the table above, we can see that increasing the parameters of the water fly mass to 165 MPa, the distance from water and object to 3 mm, the steam rate to 200 g/min, and the speed of navigation to 50 mm/min results in increases of 67.8% in MARR, 3.61% in SUR, 30.24% in KEW, and 86.86% in KEA. The proposed OFRG technique has improved 66.91% compared to the first machining.

4 Conclusion

This study analyses an AWJM method for machining OFRG composites using water fly mass, distance from water and object, steam rate, and navigation speed as inputs and MARR, SUR, KEW, and KEA as outputs. The following conclusions are drawn. Navigation speed is the most influential process parameter, contributing 60.98% of OFRG values, followed by water fly mass.

- There is a maximum improvement of 86.86% in MARR, 3.61 times improvement in SUR, 30 times improvement in KEW, and 3.61 times improvement in KEA when using the ideal parametric mix.
- Fuzzy systems demand less information to analyze an unknown process' behavior while delivering an unbiased estimate. Because fuzzy neural model generation requires minimal data, it may need to describe system dynamics fully. Fuzzy logic is used to improve the fuzzy system's capabilities. Other evolutionary algorithms often determine optimal parametric mixtures that aren't fixable in AWJM. Tuning parameters (Speed) affect the optimization performance of these methods.
- AWJM can machine thin, non-corrosive, difficult-to-cut materials. Therefore, it's used in manufacturing, coal mining, automotive, and aerospace industries. Thus, applying an artificial neuro-fuzzy method-based approach with a solid mathematical basis can enable process engineers to

Table 4 Comparison of response values

Response	Input Parametric combination	Optimal parametric combination		
		Predicted	Experimental	% of improvement
MARR	352	–	497.5	67.8
SUR	2.64	–	2.50	3.61
KEW	2.16	–	1.90	30.24
KEA	0.649	–	1.236	86.86
OFRG	0.644	0.946	0.942	66.91

derive the ideal parametric mix for the AWJM process while exploring its full cutting potential.

Acknowledgements No funding was received to conduct this study.

Declarations

Conflict of interest There are no competing interests.

References

1. Hayat, M.D., Singh, H., He, Z., Cao, P.: Titanium metal matrix composites: an overview. Compos. Part A Appl. Sci. Manuf. **121**, 418–438 (2019)
2. Li, S., Sun, B., Imai, H., Mimoto, T., Kondoh, K.: Powder metallurgy titanium metal matrix composites reinforced with carbon nanotubes and graphite. Compos. Part A Appl. Sci. Manuf. **48**, 57–66 (2013)
3. Liu, X., Liang, Z., Wen, G., Yuan, X.: Water Jet Machining and Research Developments: a Review. Int. J. Adv. Manuf. Tech. **102**, 1257–1335 (2019). https://doi.org/10.1007/s00170-018-3094-3
4. Deam, R.T., Lemma, E., Ahmed, D.H.: Modelling the abrasive water jet cutting process. Wear **257**(9–10), 877–891 (2004)
5. Cosansu, G., Cogun, C.: An investigation on using colemanite powder as abrasive in abrasive waterjet cutting (AWJC). J. Mech. Sci. Technol. **26**(8), 2371–2380 (2012)
6. Chen, F.L., Siores, E.: The effect of cutting jet variation on striation formation in abrasive water jet cutting. Int. J. Mach. Tools Manuf **41**(10), 1479–1486 (2001)
7. Natarajan, Y., Murugesan, P.K., Mohan, M., Shakeel Ahmed, L., Khan, A.: Abrasive water jet machining process: a state of art of review. J. Manuf. Process. **49**, 271–322 (2020). https://doi.org/10.1016/j.jmapro.2019.11.030
8. Jia, D.: Influence of SiC particulate size on the microstructural evolution and mechanical properties of Al–6Ti–6Nb matrix composites. Mater. Sci. Eng. A **289**, 83–90 (2000)
9. Balachandar, R., Balasundaram, R., Srinivasan, D., Raj Kumar, G.: Cut quality characteristics of Al 6061–T6 composites using abrasive water jet machining. Int. J. Mater. Eng. Innov. **9**(3), 179–194 (2020). https://doi.org/10.1504/IJMATEI.2018.096043
10. Li, J., Liu, J., Xu, C. Machinability Study of SiC Nano-Particles Reinforced Magnesium Nanocomposites During Micro-Milling Processes. In: ASME 2010 International Manufacturing Science and Engineering Conference 2010, American Society of Mechanical Engineers. pp 391–398 (2010)
11. Srinivas, S., Ramesh Babu, N.: Penetration ability of abrasive waterjets in cutting aluminum-silicon carbide particulate metal matrix composites. Mach. Sci. Technol. **16**(3), 337–354 (2012). https://doi.org/10.1080/10910344.2012.698935
12. Arul kumar, B., Kumaresan, G.: Abrasive water jet machining of aluminum-silicon carbide particulate metal matrix composites. Mater Sci Forum **830**, 83–86 (2015)
13. Niknam, S.A., Saberi, M., Kouam, J., Hashemi, R., Songmene, V., Balazinski, M.: Ultrafine and fine particle emission in turning titanium metal matrix composite (Ti-MMC). J. Cent. South Univ. **26**, 1563–1572 (2019)
14. Huang, L., Folkes, J., Kinnell, P., et al.: Mechanisms of damage initiation in a titanium alloy subjected to water droplet impact during ultra-high pressure plain waterjet erosion. J. Mater. Process. Technol. **212**, 1906–1915 (2012)
15. Thiagarajan, C., Sivaramakrishnan, R., Somasundaram, S.: Experimental evaluation of grinding forces and surface finish in cylindrical grinding of Al/SiC metal matrix composites. Proc. Inst Mech. Eng. Part B J. Eng. Manuf. **225**, 1606–1614 (2011)
16. Haghbin, N., Spelt, J.K., Papini, M.: Abrasive waterjet micromachining of channels in metals: comparison between machining in air and submerged in water. Int. J. Mach. Tool Manuf. **88**, 108–117 (2015)
17. Pramanik, A.: Developments in the non-traditional machining of particle reinforced metal matrix composites. Int. J. Mach. Tools Manuf **86**, 44–61 (2014)
18. Blau, P.J., Jolly, B.C.: Relationships between abrasive wear, hardness, and grinding characteristics of titanium-based metal-matrix composites. J. Mater. Eng. Perform. **18**, 424 (2009)
19. Parikh, P.J., Lam, S.S.: Parameter estimation for abrasive water jet machining process using neural networks. Intl. J. Adv. Manuf. Technol. **40**(5–6), 497–502 (2009)
20. Cornel, C., Emilia, C., Siliva, FP.: (2013). Neural model for abrasive water jet cutting machine, Nonconventional Technologies Review, Romanian Association of Nonconventional Technologies.
21. Rajadurai, A.: Experimental study on deep-hole making in Ti-6Al-4V by abrasive water jet machining. Mater. Res. Express **6**, 066532 (2019)
22. Hascalik, A., Çayda, U., Gürün, H.: Effect of traverse speed on abrasive waterjet machining of Ti–6Al–4V alloy. Mater. Des. **28**, 1953–1957 (2007)
23. Chaurasia, A., Wankhede, V., Chaudhari, R.: Experimental investigation of high-speed turning of INCONEL 718 using PVD-coated carbide tool under wet condition. In: Deb, D., Balas V.E., Dey, R. (eds.) Innovations in Infrastructure; Springer: Berlin/Heidelberg, Germany, 2019; pp 367–374
24. Zain, A.M., Haron, H., Sharif, S.: Review of ANN technique for modeling roughness of the cut surface performance measure in the machining process. In: Proceedings-2009 3rd Asia Intl. Conf. on Modelling and Simulation, Vol. 5071954, 35–39, AMS, (2009)
25. Yang, L., Peng, Z., Tang, C., Zhang, F.: Numerical model of abrasive water jet cutting speed based on ANN. Trans. Chin. Soc. Agric. Mach. **36**(5), 117–120 (2005)

26. Sheth, M., Gajjar, K., Jain, A., Shah, V., Patel, H., Chaudhari, R., Vora, J.: Multi-objective optimization of Inconel 718 using Combined approach of taguchi—Grey relational analysis. In: Kalamkar, K., Monkova K. (eds.) Advances in Mechanical Engineering; Springer: Berlin/Heidelberg, Germany, pp. 229–235 (2021)
27. Rathi, P., Ghiya, R., Shah, H., Srivastava, P., Patel, S., Chaudhari, R., Vora, J.: Multi-response Optimization of Ni55. 8Ti Shape Memory Alloy Using Taguchi–Grey Relational Analysis Approach. In Recent Advances in Mechanical Infrastructure; Springer: Berlin/Heidelberg, Germany, 2020; pp. 13–23.
28. Samson, R.M., Rajak, S., Kannan, T.D.B., Sampreet, K.: optimization of process parameters in abrasivewater jet machining of inconel 718 using VIKOR method. J. Inst. Eng. Series C **101**, 579–585 (2020)
29. Chakravarthy, PS., Ramesh Babu, N.: (1997). A semi empirical model for cutting granite with abrasive waterjets. Proc. of 17th AIMTDR, 259–262
30. Chakravarthy, P.S., Babu, R.N.: A hybrid approach for selection of optimal process parameters in abrasive water jet cutting. I.Mech.E. J. Eng. Manuf. Part B **214**, 781–791 (2000)
31. Ayed, Y., Germain, G.: High-pressure water-jet-assisted machining of Ti555-3 titanium alloy: investigation of tool wear mechanisms. Intl. J. Adv. Manuf. Technol. **96**, 845–856 (2018)